Scientific Reports

https://doi.org/10.1038/s41598-026-39190-3

Article in Press

KNAT7 transcription factor regulates metabolite and ion profiles to control cell wall biosynthesis in *Populus*

Received: 5 November 2025

Accepted: 3 February 2026

Published online: 17 February 2026

Cite this article as: Sharma D., Lakra N., Ahlawat Y.K. *et al.* KNAT7 transcription factor regulates metabolite and ion profiles to control cell wall biosynthesis in *Populus*. *Sci Rep* (2026). https://doi.org/10.1038/s41598-026-39190-3

Divya Sharma, Nita Lakra, Yogesh K. Ahlawat, Ajaya K. Biswal, Anurag Malik, Vishavjeet Rathee & Seid Hussein Muhie

KNAT7 Transcription Factor Regulates Metabolite and Ion Profiles to Control Cell Wall Biosynthesis in *Populus*

Divya Sharma[1], Nita Lakra[1*], Yogesh K. Ahlawat[2,3*], Ajaya K. Biswal[4,5], Anurag Malik[6], Vishavjeet Rathee[7], Seid Hussein Muhie[8*]

[1]Department of Molecular Biology & Biotechnology, College of Biotechnology, CCS Haryana Agricultural University, Hisar 125004, India
[2]Department of Life Sciences, Faculty of Allied Health Sciences, SGT University, Gurugram 122505, Haryana, India
[3]Allied Health Sciences, Datta Meghe Institute of Higher Education and Research, Wardha, Maharashtra, India
[4]Department of Biochemistry and Molecular Biology, University of Georgia, Athens, GA-30602, USA;
[5]Complex Carbohydrate Research Center, University of Georgia, Athens, GA-30602, USA
[6]Division of Research and Innovation, Uttaranchal University, Dehradun 248007, Uttarakhand, India.
[7]Department of Life Sciences, Galgotias University, Greater Noida, Uttar Pradesh, India
[8]Department of Plant Science, College of Agriculture, Wollo University, Dessie, Ethiopia

* **Correspondence**: Dr. Nita Lakra, nitalakra108@gmail.com , Dr Yogesh Ahlawat, ykahlawa@mtu.edu, and Dr. Seid Hussen Muhie, hamidashm@gmail.com

Abstract

Poplar (*Populus spp.*) is widely recognized as a fast-growing woody species with considerable potential for sustainable bioenergy production, largely due to the high cellulose content of its secondary cell walls. Members of the KNOTTED1-like homeobox transcription factor family are known regulators of plant development, and KNAT7 has been closely associated with secondary wall formation and lignification. In the present study, metabolite and ion profiles were examined in transgenic poplar lines with KNAT7 overexpression and antisense suppression to elucidate its role in metabolic regulation during wood formation. Pronounced alterations in primary metabolism were observed in KNAT7-overexpressing lines, including substantial increases in soluble sugars such as glucose, gluconic acid, mannitol, sucrose, xylitol, and cellobiose, indicating enhanced carbon allocation toward cell wall polysaccharide biosynthesis. Amino acid metabolism was also significantly affected, with elevated levels of L-glutamic acid and L-5-oxoproline, as well as increased abundance of phenylalanine and tyrosine, key precursors of the lignin biosynthetic pathway. In addition, several phenolic and defense-related secondary metabolites, including hydroquinone, resveratrol, salicylic acid, and 4-hydroxybenzoic acid, were enriched, suggesting coordinated regulation of

structural reinforcement and stress responsiveness. Elemental profiling revealed increased accumulation of Na, Mg, Fe, Mn, Zn, and Cu, with magnesium showing notable enrichment, consistent with its role as a cofactor in enzymes associated with lignin biosynthesis. Overall, the findings indicate that KNAT7 modulates metabolite and ion homeostasis in support of secondary cell wall biosynthesis, underscoring its potential utility for genetic improvement of wood quality and bioenergy-related traits in poplar.

Keywords: Transcriptional regulation; Wood formation; Metabolic reprogramming; Elemental homeostasis; Bioenergy crops

1. Introduction

Poplar (*Populus spp.*) comprises fast-growing, deciduous tree species that are widely used as model systems for woody plant biology and biotechnology due to their rapid biomass accumulation, ease of genetic manipulation, and well-annotated genomes (Zhang et al. 2019). Economically, poplars are of major importance for timber, pulp, and paper industries and are increasingly valued as renewable feedstocks for bioenergy and bio-based products, owing to their high cellulose content and favorable conversion efficiency to bioethanol (Dou et al. 2017). The yield and quality of poplar biomass are largely determined by the composition and architecture of secondary cell walls (SCWs), which are mainly composed of cellulose, hemicelluloses, and lignin.

SCW formation is a tightly coordinated developmental process controlled by complex transcriptional networks. Among the key regulators are members of the KNOTTED1-like homeobox (KNOX) transcription factor family, which play central roles in plant growth, tissue differentiation, and cell wall development (Hamant et al. 2010). KNOX proteins are broadly classified into Class I and Class II groups, with Class II KNOX genes being particularly associated with cell wall biosynthesis and vascular development. Across multiple plant species, KNOX transcription factors have been shown to influence SCW deposition by regulating genes involved in cellulose, hemicellulose, and lignin biosynthesis, as well as carbon partitioning and phenylpropanoid metabolism.

Evidence from Arabidopsis thaliana demonstrates that the Class II KNOX gene KNAT7 functions as an important regulator of SCW formation. Loss-

and gain-of-function studies have revealed that KNAT7 modulates xylan biosynthesis, lignin deposition, and cell wall thickening through interactions with NAC and MYB transcriptional networks that govern SCW regulatory hierarchies (Qin et al. 2020; Jia et al. 2024). Similar regulatory roles have been reported in other species, where KNOX family members influence lignification, vascular patterning, and mechanical strength, underscoring their conserved function in cell wall-related processes. In poplar, PtKNAT7 expression increases during stem maturation and xylem differentiation, suggesting a role in the transition from primary growth to secondary wall deposition (Li et al. 2012). Manipulation of KNAT7 expression in developing xylem has been shown to affect lignin-related gene expression and saccharification efficiency, highlighting its relevance for improving woody biomass utilization (Sahoo et al. 2014; Bryant et al. 2020).

Lignin, a phenolic polymer synthesized via the phenylalanine and tyrosine-derived phenylpropanoid pathway, represents a major structural component of SCWs and accounts for a substantial fraction of terrestrial organic carbon (Liu et al. 2018). While lignin confers mechanical strength, hydrophobicity, and stress resistance, it also contributes to biomass recalcitrance, posing a major challenge for efficient biofuel production (Yadav et al. 2023) Accordingly, extensive research has focused on transcriptional regulation of lignin biosynthesis, particularly by MYB and NAC transcription factors. NAC transcription factors such as VND6, VND7, NST1, and SND1 function as master regulators that initiate and coordinate the entire secondary cell wall transcriptional program, while MYB factors such as MYB58 and MYB63 act as downstream activators that directly and robustly induce lignin biosynthetic genes (Geng et al. 2020). In contrast, KNAT7 does not function as a primary on–off switch for secondary wall formation but instead plays a modulatory role within this regulatory hierarchy. Rather than directly driving core lignin biosynthetic pathways, KNAT7 fine-tunes secondary cell wall development by interacting with NAC–MYB networks and contributing to the balance and coordination of wall polymer deposition. This complementary role suggests that KNAT7

integrates developmental cues with metabolic regulation to adjust secondary wall composition, rather than acting as a lignin-specific transcriptional activator (Ahlawat et al. 2021). However, the extent to which KNOX transcription factors coordinate downstream metabolic fluxes and elemental requirements associated with SCW biosynthesis remains incompletely understood.

Beyond transcriptional regulation, SCW formation and lignification are fundamentally linked to cellular metabolism and ion homeostasis. Metabolomics provides a comprehensive view of primary and secondary metabolites that supply carbon skeletons and precursors for cell wall polymers, while ionomics enables high-throughput quantification of mineral nutrients and trace elements that function as enzyme cofactors and structural stabilizers (Kumar et al. 2017; Huang et al. 2016). Integration of these approaches offers a systems-level framework for understanding how transcriptional regulators translate into biochemical and physiological outcomes. Despite increasing availability of transcriptomic data on KNAT7 and related regulators, multi-omic investigations that directly connect transcription factor activity with metabolite and ion profiles in woody tissues remain limited, particularly in poplar.

Secondary cell walls represent the primary source of lignocellulosic biomass for bioenergy applications, yet their efficient conversion often requires intensive chemical pretreatments and enzymatic processing, resulting in high economic and environmental costs (Xu et al. 2017). Developing poplar genotypes with optimized metabolic composition, modified lignin biosynthesis, and balanced ion homeostasis has therefore emerged as a promising strategy to reduce biomass recalcitrance and improve biofuel production efficiency (Ragauskas et al. 2006; Bevan et al. 2006).

In this context, the present study investigates the effects of KNAT7 overexpression and antisense suppression on metabolite and ion profiles in poplar stems. By integrating metabolomic and ionomic analyses, this work provides a comprehensive assessment of how KNAT7-mediated

transcriptional regulation translates into coordinated biochemical and elemental changes associated with SCW formation. This multi-omic perspective advances current understanding of KNAT7 function beyond transcript-level regulation and offers new insights into the metabolic and ionic mechanisms underlying wood formation and biomass quality in poplar.

2. Materials and Methods

2.1 Generation of KNAT7 transgenic lines

Overexpression (OE) and antisense (AS) *KNAT7* transgenic lines were generated using the developing xylem-specific promoter DX15, which was cloned into the binary vector pBI101 via sticky-end cloning. The overexpression (sense) and suppression (antisense) constructs of the *PtKNAT7* gene were designated as *PtKNAT7*-OE and *PtKNAT7*-AS, respectively. Full-length *PtKNAT7* cDNA was amplified from poplar stem tissues using gene-specific primers containing *XbaI* and *SacI* restriction sites. The amplified fragments were cloned into the DX15pBI101 vector by replacing the *GUS* reporter gene (kindly provided by Dr. K.-H. Han, Michigan State University). For the antisense construct, the *PtKNAT7* insert was cloned in the reverse orientation relative to the sense construct. Both constructs (*PtKNAT7*-OE and *PtKNAT7*-AS) were independently introduced into hybrid poplar (*Populus tremula* × *Populus alba* clone 717-1B4) explants via *Agrobacterium tumefaciens* strain C59 using the leaf-disc transformation protocol, as previously described (Ahlawat et al. 2021, Wang et al. 2023), for the generation of independent transgenic lines. For each construct (PtKNAT7-OE and PtKNAT7-AS), three independent transgenic lines were selected, and each line was represented by three biological triplicates for metabolite profiling. WoodSamples from four-month-old transgenic poplars were used for metabolite profiling. Developing xylem was excised using a scalpel from 16-week-old greenhouse-grown plants maintained at 22°C, with samples collected from the 7th internode. This internode was selected because it represents a stage where secondary cell wall formation is clearly established, while

tissues are neither too young nor fully mature. The 7th internode has been commonly used in woody biomass studies, as it provides consistent lignification and cell wall composition, allowing reliable comparisons between samples.

2.2 Sample preparation and derivatization for metabolite profiling

Metabolite extraction was performed according to the protocol described by Fiehn (2000), using crushed woody poplar powder as the starting material. To inactivate enzymes, 700 µL of precooled methanol (-20°C) was added to 150 mg of sample in a 2 mL Eppendorf tube containing 60 µL of ribitol (0.4 mg/mL in Milli-Q water) as an internal quantitative standard. The mixture was vortexed for 10 seconds and centrifuged at 11,000×g for 15 minutes. The supernatant was transferred to a fresh 2 mL Eppendorf tube, followed by the addition of 700 µL of Milli-Q water and 370 µL of chloroform. The tube was vortexed again and centrifuged at 2,200×g for 10 minutes. The uppor polar phase was collected, dried using a vacuum concentrator, and stored at -20°C until derivatization. For derivatization, 40 µL of methoxyamine hydrochloride in pyridine (20 mg/mL) was added to the dried extract. The mixture was vortexed and incubated at 30°C for 1.5 hours on a thermomixer. Subsequently, 70 µL of N-methyl-N-(trimethylsilyl) trifluoroacetamide (MSTFA) was added to derivatize organic acids into volatile trimethylsilyl derivatives. Derivatization was used to improve the volatility and thermal stability of polar metabolites for GC–MS analysis. Methoxyamine hydrochloride stabilized carbonyl-containing metabolites by forming oxime derivatives and reducing stereoisomer formation, while MSTFA derivatized polar functional groups to enhance volatility, chromatographic separation, and detection (Fritsche-Guenther et al. 2021) The mixture was then incubated at 30°C for an additional 30 minutes (Fiehn et al. 2000).

2.3 GC–MS analysis

Gas chromatography–mass spectrometry (GC–MS) analysis was performed using an Agilent 7890A gas chromatograph equipped with an Agilent GC autosampler 120 (PAL-LHX 25 AG12) and a DB-5MS column (30 m × 0.25 mm × 0.25 µm, Agilent J&W). Helium was used as the carrier gas at a

constant flow rate of 1 mL/min in constant linear velocity mode. The oven temperature was initially set to 100°C (held for 2 min), ramped to 280°C, and held for 18 min. Samples were injected in split mode (split ratio 10:1) with an injector temperature of 260°C. Ribitol was used as a quality control standard, injected before and after each sample to monitor consistency and blanks were run between injections to avoid cross-contamination. Electron ionization at 70 eV was used as the ionization source. Metabolites were identified using the GCMS-QP2010 Ultra Shimadzu system by comparing the mass spectra against established spectral libraries such as NIST and Wiley. GCMS Postrun software was used for data analysis. Three biological replicates were collected per condition and pooled to generate one representative composite sample. From each pooled sample, three technical replicates were prepared to assess analytical precision. Statistical analysis of the GC-MS data was performed using MetaboAnalyst software (Pang et al. 2021) and origin 2024. Analysis included fold-change calculations (Significance set at $p < 0.05$, fold change > 2), principal component analysis (PCA) and heatmap clustering, to generate clustered heatmaps with optimized color schemes and high-resolution output, Python (Rossum, V. 2009) was used with the pandas (McKinney, W. 2010), and matplotlib libraries (Hunter, J. D. 2007). All datasets were evaluated for consistency and reproducibility.

2.4 Ionomic profiling in Poplar

Leaf and stem samples were collected from transgenic poplar lines overexpressing KNAT7 transcription factor (OE) and from Antisense (AS) lines. Samples were surface-washed using a 0.1 N HCl solution to remove any adhering ions, followed by through rinsing with double-distilled water. The cleaned tissues were dried in a hot air oven at 60°C until constant weight was achieved. Once dried, samples were finely powdered using a tissue lyser and stored for downstream ionomic analysis.

Leaf and stem samples were collected from transgenic poplar lines overexpressing KNAT7 transcription factor (OE) and from antisense (AS) lines. Fully expanded leaves were harvested from a consistent positional

node across all plants to ensure comparable developmental stage and physiological status. Samples from control and transgenic lines were collected from equivalent positions to maintain consistency in ionomic profiling. Tissues were surface-washed with 0.1 N HCl, thoroughly rinsed with double-distilled water, dried at 60°C to constant weight, finely powdered using a tissue lyser, and stored for downstream ionomic analysis.

2.5 Sample preparation for ICPMS

Approximately 200 mg of dried and powered tissue was weighed for digestion. Samples were subjected to microwave-assisted acid digestion using Multiwave 3000 digestion system (Anton Par) at 200℃. The digestion mixture consisted of 2.5 mL of concentrated nitric acid (HNO_3) and 1.5 mL of hydrogen peroxide (H_2O_2), following protocols adapted from Gahoonia et al. (2007). Samples were digested for 4-5 hours, cooled to at 50℃ for 30 minutes, and then filtered through Whatman filter paper followed by syringe filtration. The filtrate was diluted 10,000-fold using sterile deionized water as per Becker et al. (2008) prior to analysis. Ionome profiling was performed using an Inductively Coupled Plasma Mass spectrometry (ICP-MS) system (PerkinElmer, NexION 300X) equipped with a cross-flow nebulizer. The instrument was calibrated using a multi-element ICP solution (Sigma-Adrich). Samples were analyzed for essential macro- and micronutrients including Na, Ca, Mg, Fe, Li, Mn, B, Zn, Cu, and K. Elemental concentrations were quantified and reported in parts per million (ppm).

3. Results

3.1 Metabolome Profiling

A differential accumulation of metabolites was observed in poplar lines overexpressing (OE) and antisense (AS) KNAT7 transcription factor. Metabolites exhibiting more than a two fold change with a P-value <0.05 were considered significant, and the area percentage was calculated using MetaboAnalyst software. Wood samples were analyzed on a using GC-MS-QP2010 Ultra Shimadzu system, and data were further

processed using GC-MS Postrum. Identified metabolites were classified into major metabolic groups: sugars and sugar alcohols (Table 1, Fig. 1), amino acids (Table 1, Fig. 2), organic acids (Table 1, Fig. 3), fatty acids (Table 1, Fig. 4), and other compounds (Table 1, Fig. 5). Each analysis was performed in triplicate, and $\log_2$ fold change values were calculated to determine significant variations. Heat maps were generated using OriginPro 2024b to visualize metabolite patterns across experimental conditions

An overview of metabolites exhibiting significant changes in response to KNAT7 overexpression and antisense suppression is presented in Table 1 and provides context for the class-specific analyses described below.

Table 1. Summary of metabolite changes in wild-type and KNAT7 transgenic poplar stems.

Sugars and sugar alcohols	**OE poplar/Control**	**Control/AS poplar**	**OE poplar/AS poplar**
Xylitol	0.69	3.38	4.07
D-(+)-Cellobiose	0.67	2.91	3.59
Sucrose	1.82	1.63	3.45
Ribofuranose	0.49	2.66	3.16
D-(-)-Tagatofuranose	1.86	0.77	2.63
Turanose	0.93	1.19	2.13
Glucose	3.66	-1.88	1.78
Allose	1.67	0.10	1.77
D-Arabinose	-0.05	1.76	1.72
Maltose	1.50	-0.06	1.44
D-glucitol	0.10	0.97	1.07
D-(+)-Talose	-0.10	0.56	0.46
β-Gentiobiose	-0.22	0.56	0.34
D-(-)-Fructose	-1.96	2.20	0.24
D-(-)-Tagatose	1.89	-1.74	0.16
1,2,3-Butanetriol	0.12	0.20	0.33
L-(+)-Threose	-1.92	1.83	-0.08
Arabinose	-0.01	0.06	0.04
Mannitol	3.43	-3.41	0.02
D-Glycero-D-gulo-Heptose	0.24	-0.29	-0.05
meso-Erythritol	-0.30	0.11	-0.19
Glyceryl-glycoside	-0.64	0.03	-0.62
β-D-Lactose	0.10	-0.95	-0.85
D-Gluconic	3.32	-4.47	-1.15
Lyxofuranose	0.04	-1.67	-1.63
Glycerol	3.12	-5.57	-2.45

Melibiose	-0.01	-3.79	-3.80
Amino acids and derivatives	**OE poplar/Control**	**Control/AS poplar**	**OE poplar/AS poplar**
L-Glutamic acid	3.60	1.14	4.74
L-Proline	0.37	3.98	4.35
Serine	2.39	1.38	3.76
4-Hydroxybenzoic acid	2.82	0.84	3.66
L-5-Oxoproline	6.44	-3.35	3.09
L-Tyrosine	2.59	0.15	2.74
L-Threonine	-1.57	3.23	1.66
L-Phenylalanine	1.49	0.06	1.55
4-Aminobutanoic acid	0.94	0.52	1.46
Glycine	-1.25	2.41	1.16
L-Isoleucine	3.61	-3.49	0.11
Organic acids	**OE poplar/Control**	**Control/AS poplar**	**OE poplar/AS poplar**
4-Coumaric acid	4.14	0.00	4.14
Malic acid	3.37	0.15	3.52
2-Ketoglutaric acid	-0.37	3.06	2.69
Quininic acid	0.03	2.37	2.41
2-Butenedioic acid	0.97	0.58	1.55
Vanillic acid	0.98	-0.17	0.81
2,2-Dimethylsuccinic acid	0.33	-0.22	0.11
D-Glucuronic acid	0.17	0.09	0.26
Glyceric acid	1.88	-2.02	-0.14
Butanedioic acid	-0.32	-0.42	-0.74
2,3,4-Trihydroxybutyric acid	3.09	-3.93	-0.84
Fatty acids	**OE poplar/Control**	**Control/AS poplar**	**OE poplar/AS poplar**
Suberic acid	3.64	-0.13	3.51
Pentanedioic acid	0.45	2.84	3.29
Azelaic acid	0.08	2.53	2.61
3-Hydroxydodecanedioic acid	1.7	0.23	1.93
Oleic acid	0.9	0.18	1.07
Pimelic acid	0.36	0.44	0.81
4-Hydroxybutanoic acid	0.2	0.56	0.76
Decanoic acid	0.4	0.32	0.72
Oxalic acid	0.13	0.41	0.54
Palmitic acid	0.63	-0.19	0.45
Eicosanoic acid	0.42	-0.01	0.41
Stearic acid	0.58	-0.27	0.31
Arachidic acid	0.06	0.19	0.25

3-Hydroxyisovaleric acid	1.17	-1.46	-0.29
Other compounds	**OE poplar/Control**	**Control/AS poplar**	**OE poplar/AS poplar**
Salicylic acid	3.46	0.45	3.91
Resveratrol	4.03	-0.22	3.81
Hydroquinone	4.05	-0.35	3.70
m-Coumaric acid	2.26	0.09	2.35
p-Toluic acid	0.13	0.31	0.44
Protocatechuic acid	0.95	-0.78	0.17
Arbutin	0.05	0.04	0.09
Stigmastanol	0.05	0.07	0.12
Stigmast-5-ene	0.33	-0.26	0.08
Catechol	0.58	4.14	4.72

3.1.1 sugars and sugar alcohols

Several sugars and sugar alcohols showed accumulation patterns between KNAT7 overexpression (OE) and antisense (AS) poplar lines (Figure 1 ; Table 1). In OE plants compared with controls, glucose (log_2 fold change = 3.66), mannitol (3.43), D-gluconic acid (3.32), glycerol (3.12), and sucrose (1.82) were strongly increased. In contrast, these metabolites were markedly reduced in AS lines, including glucose (−1.88), mannitol (−3.41), D-gluconic acid (−4.47), and glycerol (−5.57

Direct comparison between OE and AS lines further confirmed this opposite regulation, with higher levels of glucose (1.78), sucrose (3.45), xylitol (4.07), and D-(+)-cellobiose (3.59) in OE plants, while glycerol (−2.45), D-gluconic acid (−1.15), and melibiose (−3.80) were lower. These results, summarized in the heatmap, indicate that KNAT7 positively regulates the accumulation of key sugars and sugar alcohols

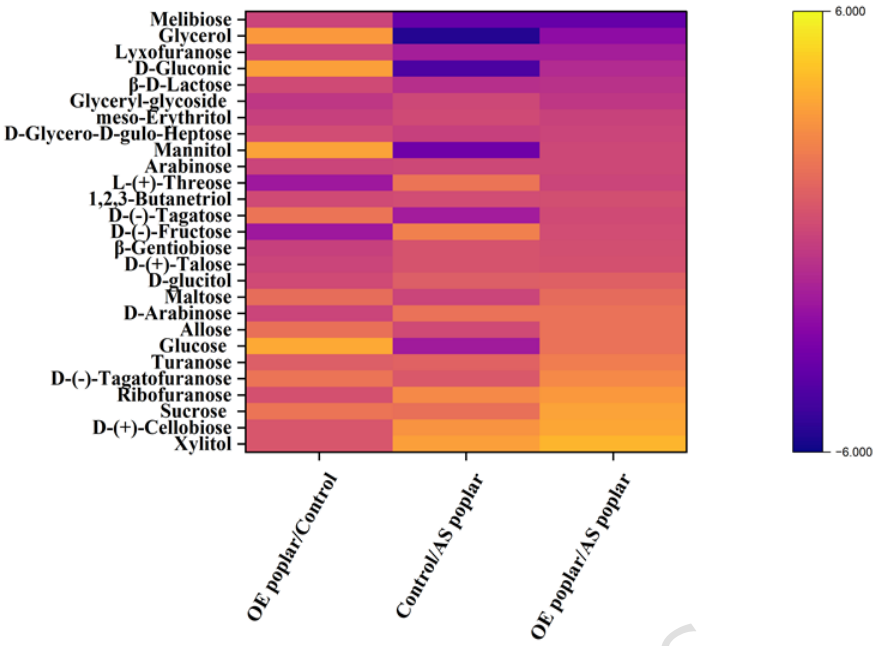

Fig. 1. Heatmap showing $\log_2$ fold changes in sugar and sugar alcohols in response to overexpression (OE) and antisense (AS) expression of the KNAT7 transcription factor in poplar. *KNAT7* is implicated in regulating genes involved in cell wall biosynthesis and modification, potentially altering sugar metabolism. Yellow indicates upregulated metabolites (positive $\log_2$ fold change), and blue indicates downregulated metabolites (negative $\log_2$ fold change)

3.1.2 Amino acids

Distinct changes in amino acid and derivative levels were observed between KNAT7 overexpression (OE) and antisense (AS) poplar lines (Figure 2; Table 1). Relative to control plants, OE lines showed increased

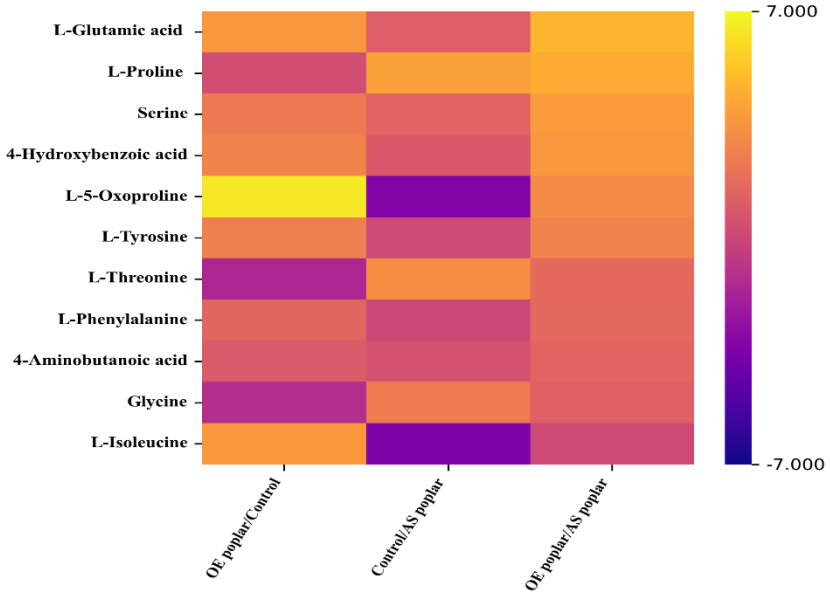

levels of L-glutamic acid (log_2 fold change = 3.60), serine (2.39), L-tyrosine (2.59), L-phenylalanine (1.49), and L-5-oxoproline (6.44), whereas L-threonine (−1.57) and glycine (−1.25) were reduced. In contrast, AS plants accumulated higher levels of L-proline (3.98), L-threonine (3.23), glycine (2.41), and serine (1.38) compared with controls, while L-5-oxoproline (−3.35) and L-isoleucine (−3.49) showed strong depletion. Direct comparison between OE and AS lines revealed higher accumulation of L-glutamic acid (4.74), L-proline (4.35), serine (3.76), and 4-hydroxybenzoic acid (3.66) in OE plants. These results indicate distinct and opposing amino acid profiles associated with KNAT7 overexpression and suppression.

Fig.2 Heatmap displaying log_2 fold changes in amino acid levels under *KNAT7* OE and AS expression. Yellow cells represent increased amino acid abundance, while blue cells indicate reduced levels relative to the control.

3.1.3 Organic acids

Several organic acids showed distinct accumulation patterns between KNAT7 overexpression (OE) and antisense (AS) poplar lines (Figure 3; Table 1). Compared with control plants, OE lines showed strong increases in 4-coumaric acid (log_2 fold change = 4.14) and malic acid (3.37), along with moderate accumulation of glyceric acid (1.88) and 2-butenedioic acid (0.97).

In contrast, AS lines exhibited higher levels of tricarboxylic acid cycle–related metabolites, including 2-ketoglutaric acid (3.06) and quinic acid (2.37), while glyceric acid (−2.02) and 2,3,4-trihydroxybutyric acid (−3.93) were markedly reduced. Direct comparison between OE and AS plants confirmed higher accumulation of 4-coumaric acid (4.14) and malic acid (3.52) in OE lines, whereas 2-ketoglutaric acid (2.69) and quinic acid (2.41) were relatively enriched in AS plants. Overall, these differences indicate that KNAT7 expression is associated with shifts in organic acid metabolism.

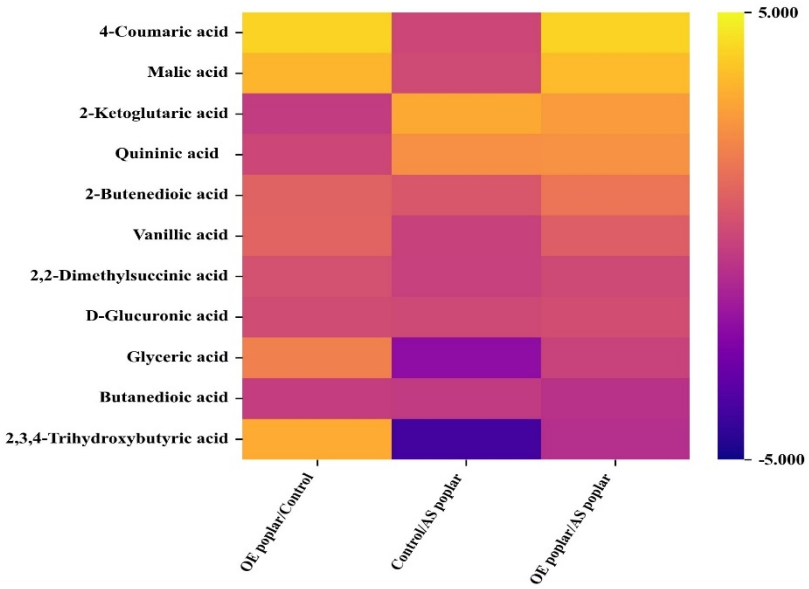

Fig. 3 Heatmap of log_2 fold changes in organic acids in response to KNAT7 OE and AS expresssion. Yellow cells denote increased organic acid content; blue cells indicate decreased abundance.

3.1.4 Fatty acids

Several fatty acids showed moderate but consistent differences between KNAT7 overexpression (OE) and antisense (AS) poplar lines (Figure 4; Table 1). Compared with control plants, OE lines showed a clear increase in suberic acid (log_2 fold change = 3.64) and a moderate rise in 3-hydroxydodecanedioic acid (1.70) and oleic acid (0.90).

In AS plants, dicarboxylic fatty acids such as pentanedioic acid (2.84) and azelaic acid (2.53) accumulated to higher levels relative to controls, whereas suberic acid showed little change (−0.13). Direct comparison between OE and AS lines confirmed higher accumulation of suberic acid (3.51), pentanedioic acid (3.29), azelaic acid (2.61), and 3-hydroxydodecanedioic acid (1.93) in OE plants. In contrast, 3-hydroxyisovaleric acid was reduced in OE compared with AS lines (−0.29).

Overall, these patterns indicate that KNAT7 influences the accumulation of specific fatty acids, particularly dicarboxylic acid–related metabolites

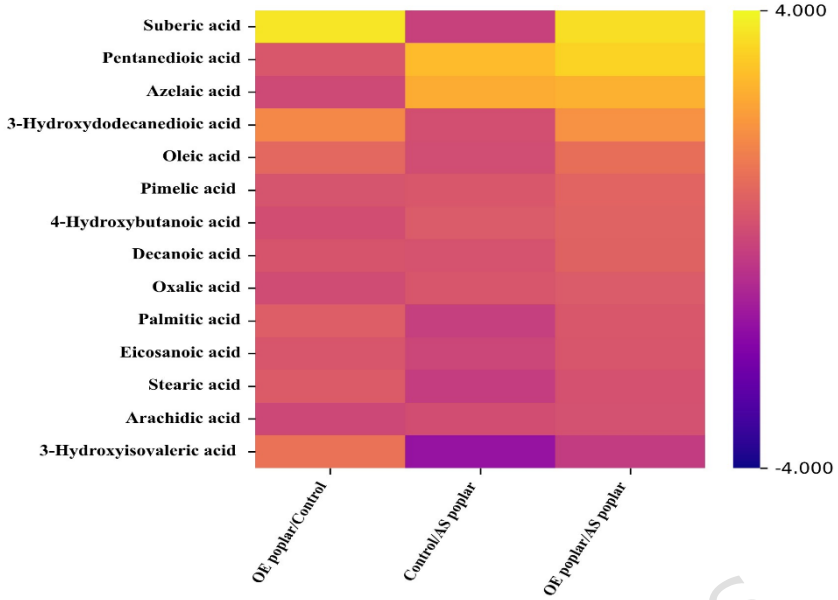

Fig. 4 Heatmap of $\log_2$ fold changes in fatty acids in response to KNAT7 OE and AS expression. Yellow cells denote increased organic acid content; blue cells indicate decreased abundance.

3.1.5 Other compounds

Several secondary metabolites showed clear differences between KNAT7 overexpression (OE) and antisense (AS) poplar lines (Figure 5; Table 1). Relative to control plants, OE lines accumulated higher levels of salicylic acid ($\log_2$ fold change = 3.46), resveratrol (4.03), hydroquinone (4.05), and m-coumaric acid (2.26), while other compounds such as p-toluic acid, arbutin, and stigmastanol showed only minor changes.

In AS plants, catechol showed a strong increase compared with controls (4.14), whereas resveratrol (−0.22) and hydroquinone (−0.35) were slightly reduced. Direct comparison between OE and AS lines confirmed substantially higher levels of salicylic acid (3.91), resveratrol (3.81), hydroquinone (3.70), m-coumaric acid (2.35), and catechol (4.72) in OE plants. Overall, these results indicate that KNAT7 overexpression is associated with enhanced accumulation of several phenolic and defense-related compounds

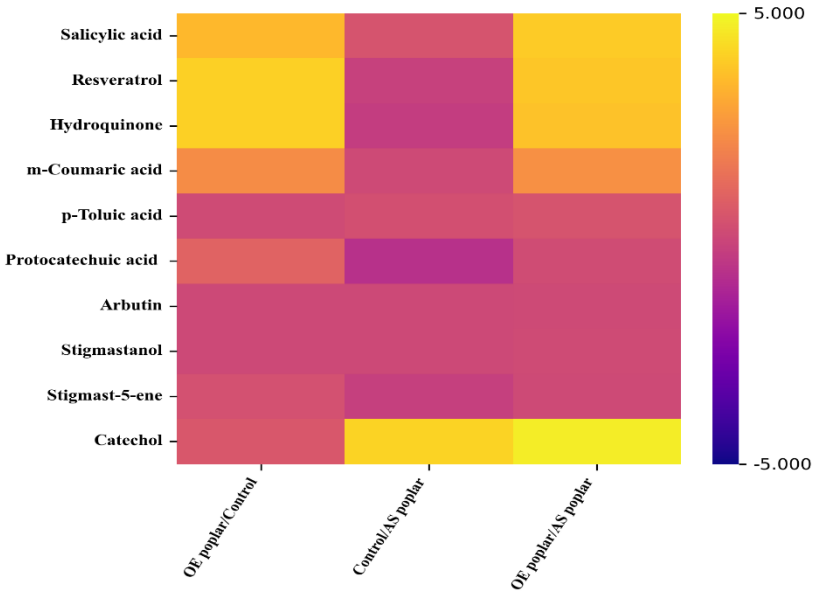

Fig. 5 Heatmap illustrating log_2 fold changes in other metabolite classes influenced by KNAT7 OE and AS expression. Yellow and blue denote increased and decreased metabolite levels, respectively

3.1.6 Differential accumulation of metabolites

A subset of selected metabolites was used to generate a heat map by using python, revealing clear differences in metabolite accumulation among control, KNAT7 TF overexpression (OE), and antisense (AS) lines in poplar. Log $_2$-fold change values were applied to construct the heatmap, where positive values indicate increased metabolite accumulation and negative value reflect reduced levels. Overexpression of KNAT7 TF resulted in significantly elevated levels of various metabolites including amino acids, sugars, and organic acids. In contrast, the antisense (AS) suppression of KNAT7 led to comparatively lower accumulation of these metabolites, underscoring the influence of KNAT7 expression on metabolic output. The observed patterns of differential metabolite accumulation are summarized in the heatmap (Figure 6).

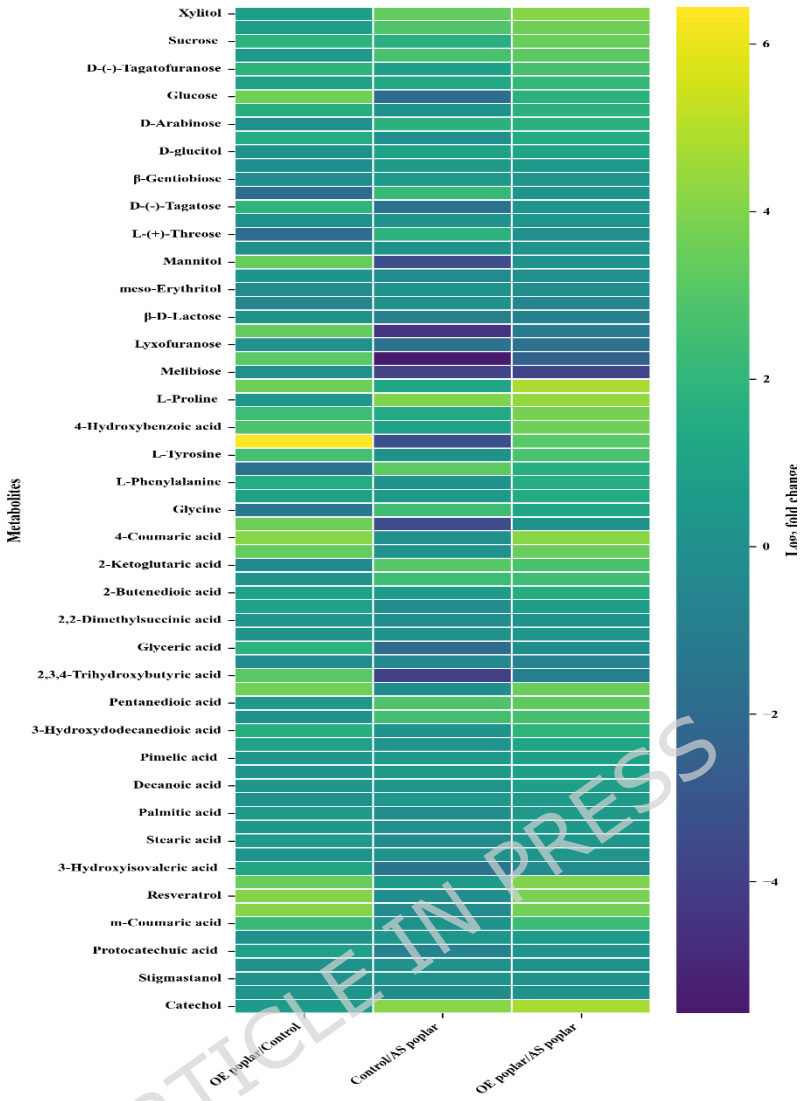

Fig. 6 Clustered heatmap depicting metabolite correlation patterns in poplar, based on Pearson distance and Ward clustering. Data are derived from partial least squares discriminant analysis (PLS-DA), with metabolite feature areas normalized and range-scaled.

3.1.7 Principal component analysis (PCA)

Principal component analysis (PCA) was performed on the metabolite data using Origin Pro 2024b. The first two principal components (PC1 and PC2) together explained 89.5% of the total variance, with PC1 (X-axis) accounting for 57.78% and PC2 (Y-axis) for 31.72%. The PCA biplot displays treatments as points and metabolites as vector, clearly distinguishing overexpression (OE), antisense (AS), and control samples. Colored points represent different group comparisons, AS poplar/Control, AS poplar/OE poplar, Control/OE poplar, and OE poplar/Control (Figure

7). PCA and hierarchical clustering provide valuable insights into the grouping and relationships among metabolites based on their variance and similarity. PCA contribution analysis revealed that OE-polar-Control was the most influential variable in defining PC2, contributing over 60% of the variance, followed by OE-polar-AS-polar. By contrast, AS-polar-Control contributed minimally, suggesting weaker differentiation along Dim-2. The PCA cluster plot identified three distinct metabolite clusters: Cluster1 (red) consisted mainly of amino acids and sugar-related metabolites such as glycine, threonine, and L-(+)-turanose; Cluster 2 (green) included glucose, serine, and malic acid, linking them to carbohydrate and organic acid metabolism; and Cluster 3 (blue) comprised glycerol, mannitol, and β-D-lactose, potentially associated with sugar alcohol metabolism. The separation along Dim1 (54.4%) and Dim2 (45.6%) suggests that these two principal components explain a significant proportion of dataset variability. Hierarchical clustering (dendrogram analysis) reinforced these groupings, revealing three major metabolite clusters (red, green, and blue) with clear hierarchical relationships. Metabolism within the same cluster exhibited closer biochemical similarity, while etween-cluster separation reflected functional distinctions. The high-level branching pattern provides valuable insights into metabolite function, which can be useful for metabolic profiling. In conclusion, PCA and hierarchical clustering highlight the key metabolites driving variability, categorize them into distinct functional groups, and provide mechanistic insight into how different metabolic pathways uniquely contribute to the observed variance, supporting biomarker discovery and metabolic profiling in poplar.

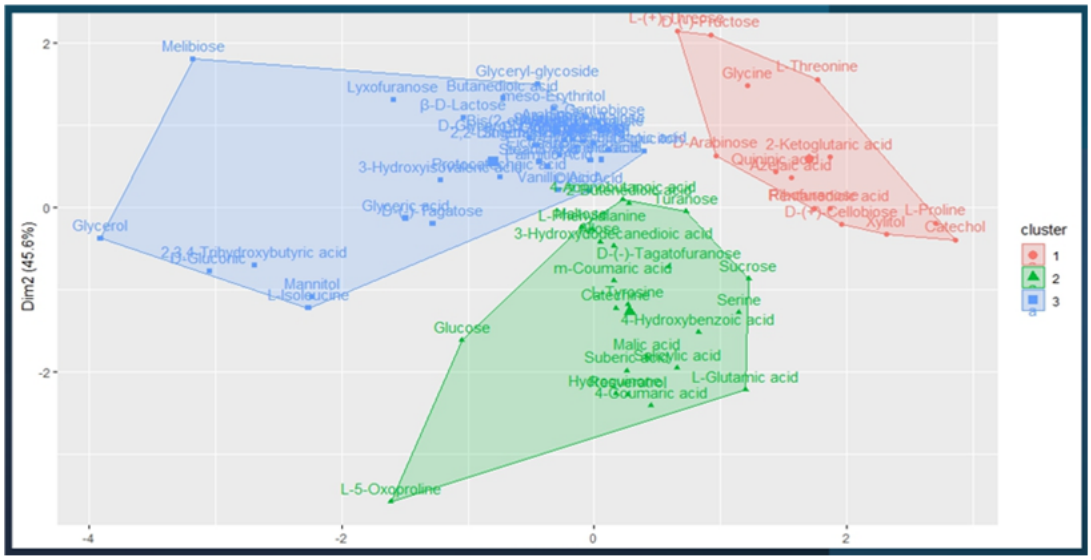

Fig. 7 Principal Component Analysis (PCA) biplot illustrating metabolic shifts under *KNAT7* OE and AS expression. Three metabolite clusters are identified: Cluster 1 (red) includes glycine, threonine, and L-(+)-turanose; Cluster 2 (green) comprises glucose, serine, and malic acid; and Cluster 3 (blue) contains glycerol, mannitol, and β-D-lactose. The PCA axes Dim1 (54.4%) and Dim2 (45.6%) explain most of the variance.

3.1.8 Metabolic Pathway Analysis

Metabolites such as Glucose, protocatechoic acid, glyceric acid, and D-glucuronic acid were more strongly associated with OE poplar/Control comparison, indicating their elevated accumulation in overexpression (OE) lines relative to control. In contrast, compounds like melibiose and glyceryl-glycoside were more closely linked with the AS poplar/control and AS poplar/OE poplar comparisons, suggesting their higher levels in antisense (AS) lines. Metabolic pathway mapping was performed using MetaboAnalyst, integrating data from KEGG database and *Arabidopsis thaliana* annotation project. In OE poplar, numerous metabolic pathways were affected, out of which only seven reaching significance ($P<0.05$) and pathway impact more than 0 (Figure 8). Notably, glycine, serine, and threonine metabolism showed the highest impact. Significant alterations were also observed in starch and sucrose metabolism, along with glyoxylate and dicarboxylate metabolism, glycerolipid metabolism, glutathione metabolism, galactose metabolism, and the biosynthesis of phenylalanine, tyrosine, and tryptophan

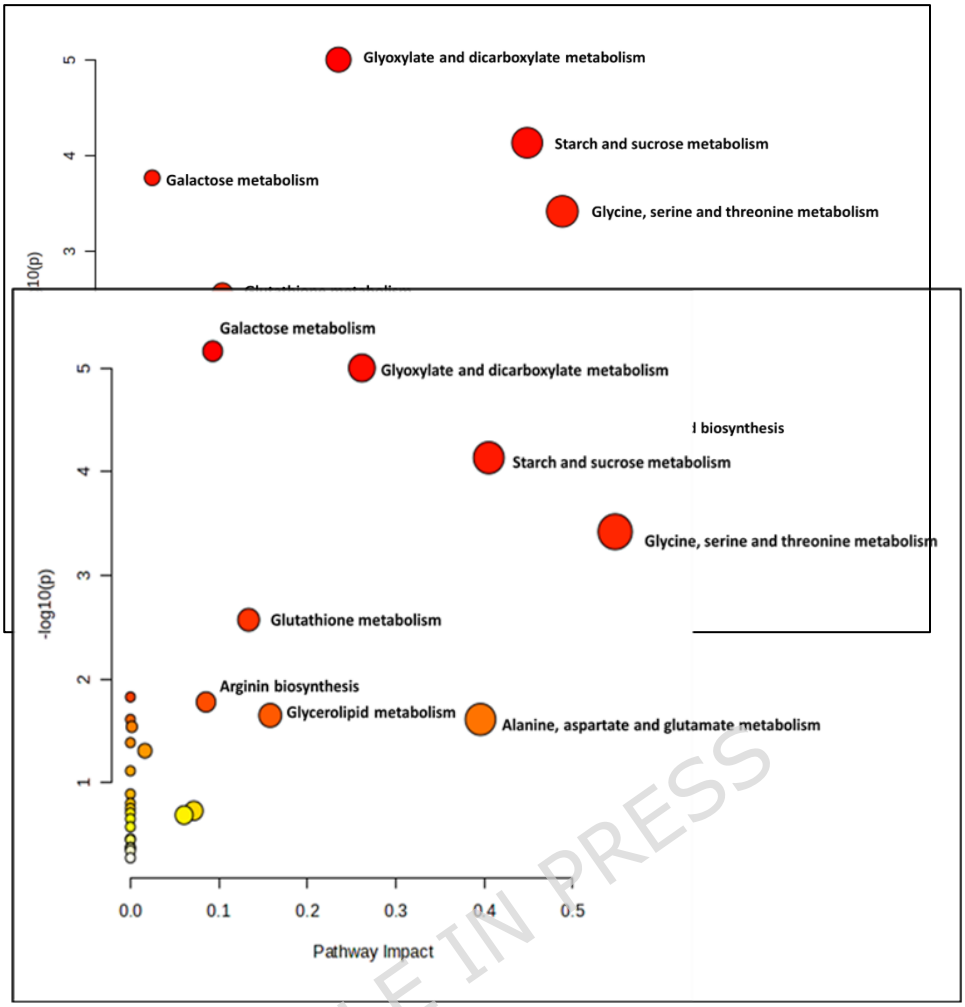

Fig. 8 Metabolome pathway impact plot highlighting pathways significantly altered in KNAT7 OE lines. The x-axis indicates pathway impact scores (0 to 1), while the y-axis displays $-\log_{10}$(p-values). High-impact pathways reflect cumulative contributions of significantly altered metabolites.

For AS poplar, ten pathways were significantly impacted (Figure 9). In addition to glycine, serine, and threonine metabolism, affected pathways included alanine, aspartate, and glutamate metabolism; glyoxylate and dicarboxylate metabolism; glycerolipid and glutathione metabolism; galactose metabolism; arginine biosynthesis; arginine and proline metabolism; and lipoic acid metabolism.

Fig. 9 Pathway impact plot for *KNAT7* AS lines, showing altered metabolic pathways. The axes represent $-\log_{10}$(p-values) versus pathway impact, with values calculated based on matched metabolite nodes

Together, these analyses demonstrate that manipulation of KNAT7 expression in poplar—via overexpression or antisense suppression

profoundly alters multiple metabolic pathways. Both OE and AS lines affect key amino acid and carbohydrate metabolism (e.g., glycine, serine, threonine, starch, and sucrose metabolism), highlighting a core regulatory role for KNAT7. However, antisense suppression appears to target nitrogen and mitochondrial-linked pathways (e.g., arginine biosynthesis, lipoic acid metabolism), whereas overexpression more strongly influences secondary metabolism, including the aromatic amino acid biosynthesis pathway. This comparative analysis underscores KNAT7's central role in coordinating primary and secondary metabolic processes that are critical for stress adaptation, nitrogen balance, and secondary cell wall biosynthesis in poplar. Several pathways, particularly those related to sugar and amino acid metabolism, were commonly affected across both genetic backgrounds, suggesting a conserved regulatory function (Table 2).

Table 2- Pathways affected by KNAT7 OE and KNAT7 AS

Pathway Name (OE)	**Pathway Name (AS)**	**Overlapped pathways**
Phenylalanine, tyrosine, and tryptophan biosynthesis	Alanine, aspartate and glutamate metabolism	Galactose metabolism
	Arginine and proline metabolism	Glutathione metabolism
	Arginine biosynthesis	Glycerolipid metabolism
	Lipoic acid metabolism	Glycine, serine and threonine metabolism
		Glyoxylate and dicarboxylate metabolism
		Starch and sucrose metabolism

3.2 Ionome profiling

The elemental composition of poplar tissues showed significant alterations in response to the overexpression (OE) and antisense (AS) regulation of the KNAT7 transcription factor (TF), relative to control plants. Magnesium (Mg) levels notably decreased in the OE lines compared to control but increased significantly in AS lines, suggesting that KNAT7 may modulate Mg homeostasis by influencing its transport or storage. Zinc (Zn)

Elements	OE/Control	Control/AS	OE/AS
Sodium	0.22	1.58	1.80
Iron	-1.76	0.63	-1.14
Manganese	2.38	-1.64	0.75
Zinc	1.04	-0.61	0.43
Boron	0.16	-0.08	0.08
Copper	1.89	-1.23	0.65
Potassium	-0.69	0.30	-0.39
Calcium	-0.37	0.17	-0.20
Magnesium	1.77	-1.14	0.63

concentrations were markedly elevated in OE lines, indicating that KNAT7 overexpression may enhance Zn uptake or reduce its utilization. Similarly, copper (Cu) levels were higher in AS lines compared to OE and control, implying a potential regulatory effect of KNAT7 on Cu transport or sequestration. Manganese (Mn) showed a strong increase in OE lines and a corresponding decrease in AS and control lines, further supporting KNAT7's role in influencing micronutrient dynamics.

Additional elemental comparisons revealed that sodium (Na) concentrations were elevated in the control relative to AS (log2 fold change 1.58), and also higher in OE compared to AS (1.80). Iron (Fe) levels were significantly increased in control versus OE (1.76), and in AS compared to OE (1.13), suggesting suppression of Fe accumulation under KNAT7 overexpression. Manganese showed the most prominent elevation in OE compared to control (2.38), while Zn and Mg levels were also elevated in OE lines, with log2 fold changes of 1.04 and 1.77, respectively. These elemental shifts, reflected in log2 fold change values, highlight how KNAT7 manipulation—either by overexpression or antisense inhibition—affects key nutrient concentrations. Such changes underscore the gene's potential involvement in nutrient acquisition, homeostasis, and stress response pathways in poplar (Table 3).

Table 3- Elements detected by ICPMS

3.2.1 Heat map analysis

A heatmap analysis was generated to visualize the log2 fold changes in elemental concentrations across control, OE, and AS poplar lines (Figure 10). Elements included in the analysis were lithium (Li), magnesium (Mg), calcium (Ca), potassium (K), copper (Cu), boron (B), zinc (Zn), manganese (Mn), iron (Fe), and sodium (Na).

Color intensity corresponds to the degree of fold change, with red indicating a positive log2 fold change (increased accumulation) and blue indicating a negative fold change (decreased accumulation) relative to the reference condition. This heatmap effectively illustrates the differential accumulation of specific elements under various genetic conditions,

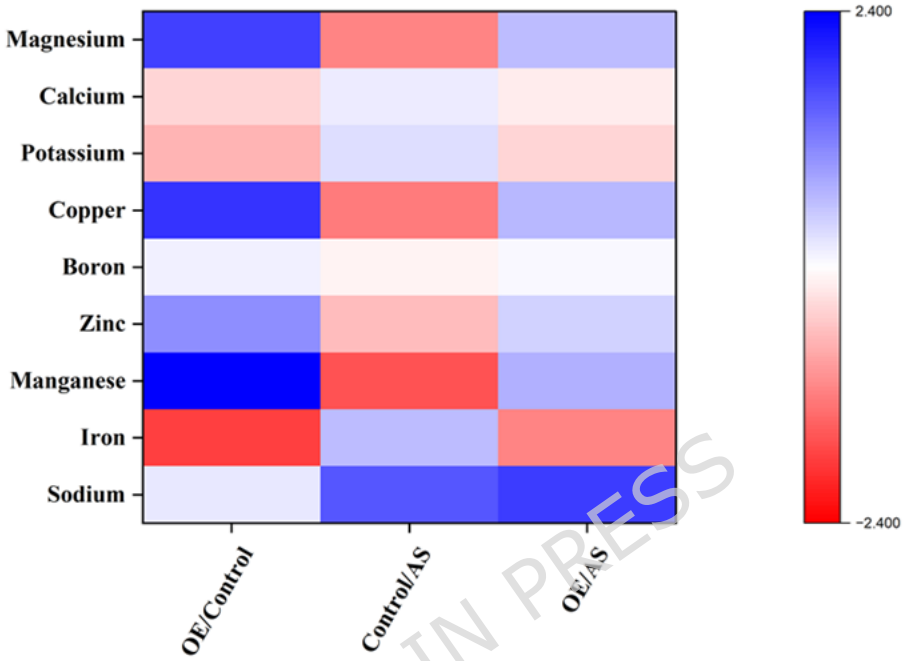

reinforcing the influence of KNAT7 on the plant's ionomic profile.

Fig. 10 ICP-MS heatmap representing log_2 fold changes in elemental composition. Red indicates increased element concentration, while blue indicates decreased levels in *KNAT7* OE and AS lines compared to control.

3.3 Phenotypic characterization of KNAT7 transgenic lines

Phenotypic effects associated with altered KNAT7 expression were assessed by comparing growth and xylem-related traits in wild-type poplars and transgenic lines with KNAT7 overexpression or antisense suppression, as reported previously (Ahlawat et al. 2021). Measurements of above-ground growth indicated that overall plant height was largely comparable between transgenic and wild-type plants, although individual overexpression and antisense lines exhibited moderate increases in height at later stages of development. In contrast, stem diameter was consistently and significantly enhanced in most KNAT7-modified lines relative to wild-type controls, indicating a measurable effect of KNAT7 manipulation on radial stem growth. Transgenic plants also produced a greater number of leaves compared with wild-type plants. Examination of stem anatomy

revealed pronounced and quantifiable differences in xylem development among genotypes. PtKNAT7 overexpression lines exhibited an approximately 15% reduction in xylem area compared with wild-type plants, whereas PtKNAT7 antisense lines showed a substantial ~26% increase in xylem area. In contrast, heterologous AtKNAT7 overexpression lines showed a more moderate ~13% increase in xylem area relative to wild-type controls. These anatomical differences were supported by representative whole-plant images and stem cross-sections reported in the referenced study. Statistical analyses confirmed that the observed variations in growth parameters and xylem traits between KNAT7 transgenic and wild-type lines were significant, demonstrating that modulation of KNAT7 expression is associated with distinct phenotypic outcomes related to secondary xylem development and wood formation (Ahlawat et al. 2021).

3.4 Correlation between phenotypic traits and metabolic profiles

To examine the relationship between phenotypic traits and underlying biochemical changes associated with KNAT7 manipulation, growth- and xylem-related parameters were evaluated alongside alterations in lignin composition and saccharification-related metabolic outputs, as previously reported (Ahlawat et al. 2021). Distinct associations were observed between xylem development, lignin characteristics, and sugar release efficiency across KNAT7 overexpression and antisense lines, indicating coordinated regulation of secondary cell wall traits and downstream metabolic outcomes.

KNAT7 antisense lines, which exhibited an approximately 26% increase in xylem area, showed a concomitant ~6% reduction in total lignin content and a marked 8–12% increase in the syringyl/guaiacyl (S/G) lignin ratio relative to wild-type plants. These structural and compositional changes were associated with substantial enhancements in saccharification efficiency, with glucose release increasing by 44–53% and xylose release by 55–67% compared to wild-type controls. In contrast, PtKNAT7 overexpression lines displayed a ~15% reduction in xylem area, no significant change in total lignin content, but a 5–7% increase in S/G ratio,

accompanied by more moderate increases in sugar release (22–26% for glucose and 28–34% for xylose). AtKNAT7 overexpression lines showed an intermediate phenotype, with a ~13% increase in xylem area, elevated S/G ratios, and 24–30% increases in glucose release.

Collectively, these results demonstrate a clear relationship between altered xylem development, lignin composition, and downstream metabolic performance. Increased xylem expansion and higher S/G lignin ratios were associated with reduced biomass recalcitrance and enhanced sugar release, whereas reduced xylem area and more modest lignin modifications corresponded to comparatively lower gains in saccharification efficiency.

4. Discussion

KNAT7 as a Central Regulator of Secondary Cell Wall–Associated Metabolism

This study investigated how overexpression and antisense knockdown of the KNAT7 transcription factor affect metabolite and ion profiles in poplar. KNAT7 plays a central role in the regulation of secondary cell wall biosynthesis, an essential process for plant structural integrity and biomass accumulation. Through, genetic manipulation of KNAT7, we observed significant alterations in the levels of key metabolites, including sugars, amino acids, and fatty acids. These shifts suggest that *KNAT7* modulates metabolic pathways linked to cell wall development and broader physiological functions. In addition to metabolite profiling, we performed ionomic analysis to evaluate changes in elemental composition. Elements such as calcium and magnesium, which are critical for cell wall cross-linking and structural stability, showed altered accumulation in response to KNAT7 expression changes. These ionomic shifts underscore the integrative role of KNAT7 in coordinating both metabolic and ionic processes that support cell wall biosynthesis and plant stress response. By combining metabolomics and ionomics, this work provides a systems-level perspective on how KNAT7 regulates plant metabolism and nutrient homeostasis. The insights gained here have implications for enhancing biomass quality and quantity in poplar a key feedstock for bioenergy and

bioproduct applications. Targeting KNAT7 and its downstream pathways may offer a promising strategy for engineering trees with improved cell wall characteristics and resource-use efficiency. These results supports a central role of KNAT7 as a central coordinator linking secondary cell wall formation with broader metabolic and ionic processes in poplar.

Integration of KNAT7 with Known Secondary Cell Wall Regulatory Networks

In *Arabidopsis thaliana*, the transcription factors KNAT7 and MYB75 have been shown to interact both in yeast two-hybrid assays and in vivo. Both proteins are essential for secondary cell wall formation in stems and seed coats. Transcript analysis and scanning electron microscopy (SEM) have confirmed their involvement, along with their interactions with each other seed coat regulators. These findings suggest that MYB75 functions within a conserved regulatory complex that modulates cell wall biosynthesis (Ahlawat et al. 2021).

Similar to our observations, other transcription factors have been implicated in regulating secondary wall biosynthesis and wood formation. NAC transcription factors are well established as regulators of secondary cell wall development. Yao et al. (2020) reported that NAC15 promotes wood formation through direct activation of genes involved in lignin and cellulose biosynthesis. By contrast, KNAT7 overexpression in our study was associated with increased levels of sugars, amino acids, and other secondary metabolites that supply substrates for cell wall construction. While NAC15 appears to function primarily through direct transcriptional activation of structural biosynthetic genes, our KNAT7 overexpression lines exhibited significant accumulation of sugars, amino acids, and secondary metabolites that serve as precursors for cell wall assembly. These findings point to complementary regulatory strategies by which transcription factors enhance wood production, either by transcriptional control of biosynthetic pathways (e.g., NAC15) or by reprogramming metabolic fluxes and ion homeostasis (e.g., KNAT7).

Previous transcriptomic studies of *KNAT7* overexpression and knockout lines further support its central role in secondary cell wall (SCW)

regulation. In poplar lines overexpressing *KNAT7*, specifically *PtKNAT7-OE* and *AtKNAT7-OE*, numerous downstream genes involved in SCW biosynthesis were significantly upregulated compared to wild-type (WT) controls. This transcriptional activation was associated with enhanced secondary wall formation, consistent with the findings of the present study. Conversely, in the *PtKNAT7*-AS lines, where *KNAT7* expression is reduced, there was a marked downregulation of SCW-related genes. This decrease in gene expression coincided with reduced lignin content in the wood, further highlighting the critical regulatory role of *KNAT7* in lignin biosynthesis and SCW development. These observations underscore *KNAT7* as a transcriptional modulator of secondary wall gene networks, directly influencing the structural integrity and biomass productivity of poplar (Wang et al. 2019).

Metabolic Reprogramming Supports Enhanced Cell Wall Biosynthesis

The pathway enrichment analysis highlights the role of KNAT7 in linking secondary cell wall biosynthesis with wider metabolic processes. In KNAT7 overexpression (OE) lines, the significant enrichment of phenylpropanoid and carbohydrate metabolism pathways indicates an increased demand for lignin precursors and structural carbohydrates required for secondary wall formation (Xu et al. 2023). In contrast, antisense (AS) lines preferentially showed enrichment of stress- and defense-related pathways, likely reflecting metabolic imbalance associated with compromised cell wall integrity. Similar shifts have been reported in secondary wall–defective mutants, underscoring the close relationship between cell wall formation, stress signaling, and metabolic homeostasis (Yamaguchi et al. 2025).

Consistent with these pathway-level changes, KNAT7 overexpression resulted in elevated levels of several amino acids and related metabolites, including, 4-aminobutanoic acid, 4-hydroxybenzoic acid, glycine, L-5-oxoproline, L-glutamic acid, L-phenylalanine, L-proline, L-threonine, L-tyrosine, serine, and L-isoleucine. These compounds play critical roles in primary metabolism, stress adaptation, and secondary cell wall

biosynthesis. For example, 4-aminobutanoic acid (GABA) functions as a key signaling molecule under abiotic stress conditions and is involved in nitrogen-carbon balance and redox regulation (Heli et al. 2022).

Similarly, 4-hydroxybenzoic acid is a precursor for lignin biosynthesis, directly contributing to the formation and structural reinforcement of cell walls (Mottiar et al. 2023). Core amino acids such as glycine, glutamic acid, and phenylalanine are central to protein synthesis and metabolic flux control. Notably, L-phenylalanine also serves as a direct precursor in the phenylpropanoid pathway, driving lignin and flavonoid biosynthesis (Pratelli et al. 2014). The enhanced accumulation of these metabolites in KNAT7-overexpressing lines suggests a transcriptionally driven upregulation of biosynthetic pathways involved in structural polymer formation and stress resilience. This metabolic reprogramming is likely to contribute to improved cell wall deposition, increased biomass yield, and enhanced stress tolerance, traits desirable for bioenergy and biomaterial feedstocks. These findings underscore the potential of targeting transcription factors such as *KNAT7* to optimize plant growth, metabolic efficiency, and downstream industrial applications.

Our findings align with previous reports indicating that KNAT7 indirectly modulates phenylpropanoid metabolism by regulating precursor flux through the shikimate and phenylpropanoid pathways, thereby influencing lignin composition and structure (Pascula et al. 2016). In addition, alterations in fatty acid and lipid profiles observed in KNAT7-modified lines point to a potential role for KNAT7 in membrane-associated lignification processes (Cao et al. 2024), further supporting its involvement in secondary wall assembly.

Similar findings were reported in a recent study investigating the role of lignin as a major structural component of plant vascular tissues (Zhu et al. 2024). Lignin, a complex polymer derived from phenylpropanoids, is synthesized through pathways that depend on the aromatic amino acid phenylalanine (Phe), which serves as a precursor for various secondary metabolites, including lignins and flavonoids. In that study, Geng and colleagues identified several MYB transcription factors (MYB20, MYB42,

MYB43, and MYB85) that directly activate genes involved in both lignin and phenylalanine biosynthesis during secondary cell wall formation in *Arabidopsis thaliana*. These MYBs were shown to play a critical role in coordinating the metabolic and biosynthetic pathways essential for vascular integrity and function. Their work complements the current findings on *KNAT7* overexpression, further underscoring the importance of transcriptional regulation in secondary cell wall biosynthesis.

Another study demonstrated that nitrogen (N) availability plays a pivotal role in regulating carbon (C) and nitrogen metabolism, which in turn significantly affects lignin and cellulose production in poplar wood (Zhao et al., 2014). Under low nitrogen (LN) conditions, an increase in lignin, soluble sugars, and starch was observed, accompanied by a reduction in cellulose content, protein levels, and free amino acids. These physiological changes were also associated with thicker fiber cell walls and a lower syringyl/guaiacyl (S/G) lignin ratio. Metabolite and transcriptomic analyses revealed that the phenylpropanoid pathway was notably influenced, with elevated levels of intermediates such as cinnamic acid and caffeic aldehyde, alongside the upregulation of key biosynthetic genes including *PAL*, *HCT*, and *CAD*. These findings underscore how nitrogen limitation can redirect carbon fluxes toward lignin biosynthesis and affect cell wall composition, offering valuable insights into how nutrient availability can be leveraged to optimize wood quality and enhance carbon sequestration through genetic or silvicultural strategies.

Similar trends were observed in the present study, where overexpression of *KNAT7* led to the upregulation of metabolites involved in lignin biosynthesis and pathways associated with structural integrity. The increased production of lignin and other structural components contributed to improved mechanical strength and greater biomass accumulation in *Populus* plants. Collectively, these findings reinforce the role of *KNAT7* as a key transcriptional regulator of secondary cell wall metabolism. Together with previous studies, our results underscore the importance of metabolic regulation in optimizing lignin and cellulose biosynthesis, offering promising avenues for engineering wood

composition and boosting biomass yields for bioenergy and bioproduct applications.

A recent study identified two lignin biosynthesis-related genes, KNAT7 and CRL2, as central hub genes within the phenylpropanoid biosynthetic pathway. In *Arabidopsis thaliana*, KNAT3 and KNAT7 were shown to act synergistically to promote the synthesis of syringyl (S)-lignin and regulate secondary cell wall development. In addition, five associated transcription factor genes, GLABRA3, MYBD, MYB4, MYB7, and MYB111, exhibited high expression levels in stem tissues, underscoring their potential regulatory roles in phenylpropanoid metabolism. Phenylalanine, the upstream precursor in this pathway, plays a pivotal role in lignin biosynthesis, thus linking primary metabolic flux to the formation of structural components critical for plant vascular integrity (Qin et al. 2020).

In the present study overexpression of KNAT7 in poplar stem wood revealed its significant influence on aromatic amino acid metabolism, particularly the biosynthesis of phenylalanine, tyrosine, and tryptophan. Elevated levels of these metabolites, including phenylalanine, a key precursor for lignin biosynthesis, underscore the role of KNAT7 in enhancing metabolic activities associated with secondary cell wall formation.

KNAT7 Links Metabolic Flux with Ion Homeostasis

Previous studies indicate that lignin biosynthesis is closely linked to ion homeostasis, as monolignol polymerization requires redox-active metals such as Fe^{2+} and Mn^{2+} (Huang et al. 2019).

Potassium (K^+) is the principal cation in trees, essential for maintaining cell turgor and regulating the intracellular ionic environment. It is absorbed by roots, loaded into the xylem, and transported into the aerial part through a coordinated network of potassium channels and transporters (Chevilly et al. 2021). Sodium (Na^+) competes with potassium for uptake, and the K^+/Na^+ ratio is widely recognized as an indicator of a plant's tolerance to salt stress (Chevilly et al. 2021; Wang et al. 2021). In our study, modulation of KNAT7 expression resulted in altered potassium and sodium levels, suggesting a regulatory role for this transcription factor

in ion homeostasis. This suggests that the possibility that KNAT7 engineered poplar lines could exhibit improved performance under salt stress conditions. However, we cannot rule out the possibility that these effects on cation homeostasis are indirect. Given that sugar metabolism is known to influence potassium uptake in model systems, it is plausible that the observed ionomic shifts stem from broader metabolic reprogramming driven by KNAT7 activity (Huang et al. 2019).

Further, the overexpression of the KNAT7 transcription factor (KNAT7TF) led to a significant increase in magnesium (Mg^{2+}) ion levels compared to both control and antisense groups. This observation suggests that KNAT7TF may play a regulatory role in magnesium ion homeostasis within plant cells. Elevated magnesium levels in the overexpression group could have important implications for lignin biosynthesis, as magnesium serves as a cofactor for several key enzymes involved in the phenylpropanoid and shikimate pathways. These pathways contribute to the production of lignin precursors, highlighting a potential mechanistic link between transcriptional regulation by KNAT7 and enhanced secondary cell wall formation through modulation of mineral nutrition and enzyme activity.

A study demonstrated that reduced magnesium content in roots adversely affected lignin deposition in the protoxylem and endodermal cell walls within the root differentiation zone of *Citrus sinensis* (Ye et al. 2021). Magnesium deficiency led to insufficient lignification of the Casparian strip and xylem cell walls, likely impairing the efficiency of xylem-mediated nutrient loading. As a result, nutrient transport to above-ground plant parts were diminished, ultimately inhibiting overall plant growth and development. These findings highlight the critical role of magnesium in lignin biosynthesis and structural integrity of plant cell walls. Magnesium deficiency disrupts the lignification process, resulting in weaker cell walls that compromise nutrient transport and mechanical strength (Ahmed et al. 2023). This underscores the importance of magnesium in supporting essential physiological processes required for robust plant development and growth.

The overexpression of the KNAT7 transcription factor (KNAT7TF) resulted in a marked increase in copper (Cu) ion levels when compared to both control and antisense lines. This elevation suggests a potential regulatory role of KNAT7TF in copper homeostasis. Copper is an essential micronutrient involved in redox reactions, lignin polymerization, and plant defense responses, and its accumulation may contribute to enhanced structural integrity and stress resilience. In addition, magnesium, a key cofactor in chlorophyll biosynthesis, photosynthesis, and enzyme activation, was also significantly elevated in the overexpression lines. Magnesium plays a critical role in activating enzymes responsible for the biosynthesis of phenolic compounds, which serve as precursors for lignin synthesis (Mydy et al. 2021). A reduction in magnesium impairs these enzymatic activities, potentially reducing lignin deposition and weakening cell wall structure. Conversely, elevated magnesium levels may promote lignin biosynthesis, thereby enhancing cell wall strength and improving tolerance to abiotic stresses such as drought or salinity (Barros et al. 2015).

Copper is a vital micronutrient and serves as an essential cofactor for a range of enzymes involved in oxidative processes in plants. Enzymes such as laccases and peroxidases, which are key to lignin polymerization, require copper for their catalytic activity (Chigumba et al. 2022). Copper also supports the function of superoxide dismutases (SODs), which protect plant cells from oxidative damage during environmental stress (Marschner, 2011). Alterations in copper concentrations can directly influence the lignin biosynthesis. A deficiency in copper may impair the activity of lignin-polymerizing enzymes, leading to defective cell wall formation and compromised structural integrity. This may render plants more susceptible to abiotic and biotic stresses. Conversely, excessive copper can induce toxicity by promoting oxidative stress and damaging cellular components, further disrupting cell wall development (Sharma et al. 2021).

Beyond its role in lignin formation, copper is critical for various metabolic pathways, including the biosynthesis of alkaloids, flavonoids, lignans, and

cyclic peptides compounds essential for plant defense and development (Xu et al. 2024). These findings underscore copper's multifaceted importance in plant biochemistry and its broader impact on growth, stress tolerance, and structural resilience.

Implications for Stress Tolerance

Research has shown that genes involved in secondary cell wall biosynthesis, such as KNAT7, are closely associated with plant stress tolerance mechanisms (Zhong et al., 2010). For instance, overexpression of KNAT7 may enhance a plant's ability to withstand abiotic stresses by reinforcing the structural integrity of the cell wall an important trait under conditions such as drought or high salinity (Liu et al. 2014). Secondary cell wall plays a key role in maintaining turgor pressure and protecting cellular components during stress, contributing to enhanced resilience under adverse environmental conditions (Ma et al. 2023). In addition to KNAT7, other transcription factors including members of the MYB family and NAC domain-containing proteins have been implicated in the regulation of stress-responsive genes (Gall et al. 2015). Notably, previous studies have reported that an increase in sugar levels or metabolites associated with glycolysis correlates with improved abiotic stress tolerance (Huang et al. 2019; Benito et al. 2023). Our current findings support this observation, as the overexpression of KNAT7 was accompanied by elevated levels of sugars and glycolysis-related metabolites, suggesting a metabolically driven enhancement of stress tolerance mechanisms.

In contrast, the knockdown of KNAT7 may compromise the plant's ability to adapt to environmental stress by weakening cell wall integrity, thereby increasing susceptibility to damage under drought or salinity conditions (Munns et al. 2008). Given KNAT7*'s* involvement in cell wall regulation and ion homeostasis, its downregulation could impair the expression or function of ion transporters critical for maintaining osmotic balance during stress. This suggests a broader role for KNAT7 in modulating ionic fluxes and signaling pathways associated with abiotic stress tolerance (Taïbi et al. 2017).

Relevance for Biomass Improvement and Bioenergy Applications

From an applied point of view, the ion changes seen after modifying KNAT7 suggest practical ways to improve poplar as a bioenergy crop. Changes in elements such as magnesium, calcium, potassium, and copper can affect cell wall structure, lignin formation, and the activity of enzymes involved in carbohydrate and phenylpropanoid metabolism. Higher magnesium levels may support enzymes that produce lignin precursors, which could make biomass easier to process during chemical or enzymatic conversion. Proper calcium and potassium balance helps maintain cell wall strength, water balance, and tolerance to stresses such as drought and salinity (Heise et al. 2021) Copper levels may also influence lignin formation through enzymes like laccases and peroxidases that are involved in secondary cell wall development (Chen et al. 2002) Overall, these results suggest that regulating ion balance through KNAT7 could help improve both biomass processing efficiency and stress tolerance in poplar, increasing its usefulness as a bioenergy crop.(Xie et al. 2025)

We acknowledge that a key limitation of our study is its confinement to greenhouse conditions, which may not fully replicate field environments. However, previous research has demonstrated that greenhouse studies are valuable for investigating woody plants at the molecular and metabolic levels, as they allow for tight control of environmental variables. In contrast, field conditions are subject to numerous uncontrollable factors that can introduce variability. Thus, controlled greenhouse experiments provide critical baseline data on the effects of specific variables, though it is essential to validate these findings under natural field conditions. Future research will focus on evaluating the biotechnological potential of the transgenic lines described in this study, with particular attention to their performance in field trials.

5. Conclusions

This study underscores the pivotal role of the KNAT7 transcription factor in regulating carbohydrate metabolism, secondary metabolite biosynthesis, and stress responses in poplar, a key feedstock for second-generation biofuels. Overexpression of KNAT7 significantly reprograms

metabolic pathways, leading to increased accumulation of sugars, amino acids, organic acids, fatty acids, and specialized metabolites, along with notable alterations in the plant ionome. In contrast, antisense suppression of KNAT7 disrupts these pathways, particularly reducing metabolite levels associated with amino acid and lipid metabolism. Together, these findings position KNAT7 as a promising biotechnological target for enhancing biomass yield, metabolite production, and abiotic stress resilience, key traits for improving poplar's utility as a sustainable bioenergy crop (Figure 11).

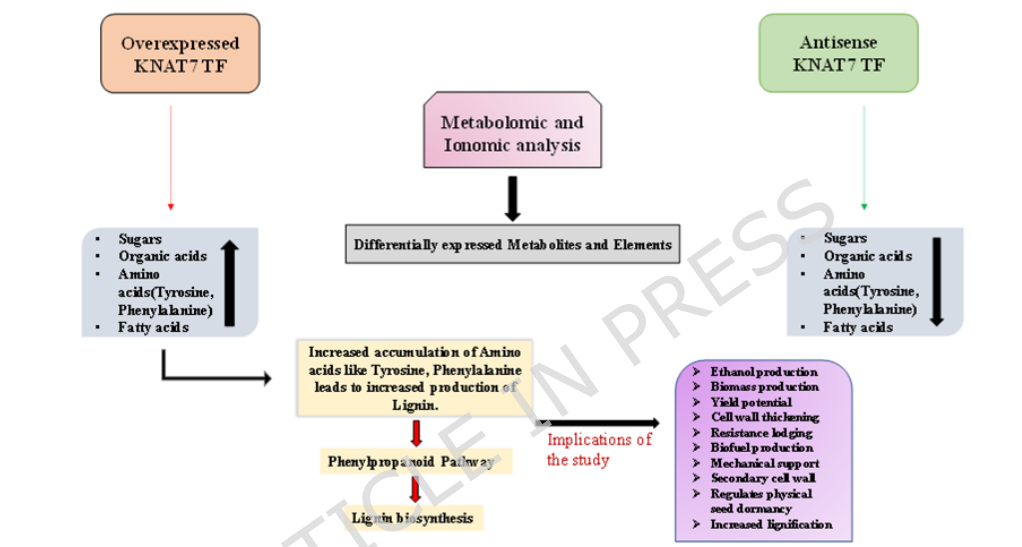

Fig. 11 Schematic model summarizing the role of KNAT7 in regulating metabolite and ion profiles in poplar. KNAT7 overexpression enhances the accumulation of sugars, organic acids, amino acids (mainly tyrosine and phenylalanine), and fatty acids, promoting phenylpropanoid pathway and lignin biosynthesis. These changes contribute to improved biomass-related traits. In contrast, antisense suppression of KNAT7 reduces metabolite accumulation, indicating disruption of associated metabolic pathways.

Acknowledgments: N/A

Author Contributions

Conceptualization: Divya Sharma, Yogesh K. Ahlawat, and Seid Hussen Muhie. **Data curation:** Divya Sharma, Nita Lakra**, Funding acquisition**: ; **Investigation:** Yogesh K. Ahlawat, Nita Lakra, **Methodology:** Divya Sharma, Yogesh K. Ahlawat, Nita Lakra, **Resources**: Divya Sharma, Yogesh K. Ahlawat, Nita Lakra, **Software:** Divya Sharma, Yogesh K. Ahlawat, Nita Lakra. **Writing – original draft**: Divya Sharma, Yogesh K. Ahlawat, Nita Lakra, and Seid Hussen Muhie. **Writing – review & editing:** Divya Sharma, Yogesh K. Ahlawat, Nita Lakra, Anurag Malik, Vishavjeet Rathee, Ajaya K. Biswal and Seid Hussen Muhie

Funding: Did not receive any funding for the research

Data Availability of data and materials: The data supporting the findings are accessible both within the paper and in the supplementary materials available online.

Declaration
Conflicts of Interest: The authors declare no conflict of interest

Acknowledgement: N/A

Ethics approval: Plant Material: We confirm that all necessary permissions and licenses were obtained for the collection of *Populus* samples used in this study. The collection was conducted in compliance with local, national, and international regulations governing plant specimen collection and research.The plant specimens were identified as hybrid poplar 717 and are not a restricted species and the identification details have been properly documented in the manuscript.

References

1. Ahlawat, Y.K., Nookaraju, A., Harman-Ware, A.E., Doeppke, C., Biswal, A.K., Joshi, C.P., 2021. Genetic modification of KNAT7 transcription factor expression enhances saccharification and reduces recalcitrance of woody biomass in poplars. Frontiers in Plant Science 12, 762067.
2. Ahmed, N., Zhang, B., Bozdar, B., Chachar, S., Rai, M., Li, J., Li, Y., Hayat, F., Chachar, Z., Tu, P., 2023. The power of magnesium: unlocking the potential for increased yield, quality, and stress tolerance of horticultural crops. Frontiers in plant science 14, 1285512.
3. Barros, J., Serk, H., Granlund, I., Pesquet, E., 2015. The cell biology of lignification in higher plants. Annals of botany 115, 1053-1074.
4. Becker, A.M., Gerstmann, S., Frank, H., 2008. Perfluorooctanoic acid and perfluorooctane sulfonate in the sediment of the Roter Main river, Bayreuth, Germany. Environmental Pollution 156, 818-820.
5. Benito, P., Bellón, J., Porcel, R., Yenush, L., Mulet, J.M., 2023. The biostimulant, potassium humate ameliorates abiotic stress in Arabidopsis thaliana by increasing starch availability. International Journal of Molecular Sciences 24, 12140
6. Bevan, M.W., Franssen, M.C., 2006. Investing in green and white biotech. Nature biotechnology. 24, 765-767.
7. Bryant, N.D., Pu, Y., Tschaplinski, T.J., Tuskan, G.A., Muchero, W., Kalluri, U.C., Yoo, C.G., Ragauskas, A.J., 2020. Transgenic poplar designed for biofuels. Trends in plant science 25, 881-896.
8. Cao, L., Zhang, S., Cao, J., Chang, R., Qu, C., Li, C., Yan, J., Quan, X., Xu, Z., Liu, G., 2024. Nitrogen modifies wood composition in poplar seedlings by regulating carbon and nitrogen metabolism. Industrial Crops and Products 219, 119118.

9. Chen, E. L., Chen, Y. A., Chen, L. M., Liu, Z. H., 2002. Effect of copper on peroxidase activity and lignin content in *Raphanus sativus*. Plant Physiology and Biochemistry 40, 439-444
10. Chen, S., Ma, F., Chen, J., Qi, M., Wei, Q., Tao, Z., Sun, B., 2025. Function of R2R3-type Myeloblastosis Transcription Factors in Plants. Rice Science 32, 307-321
11. Chevilly, S., Dolz-Edo, L., Martínez-Sánchez, G., Morcillo, L., Vilagrosa, A., López-Nicolás, J.M., Blanca, J., Yenush, L., Mulet, J.M., 2021. Distinctive traits for drought and salt stress tolerance in melon (Cucumis melo L.). Frontiers in Plant Science 12, 777060.
12. Chevilly, S., Dolz-Edo, L., Morcillo, L., Vilagrosa, A., López-Nicolás, J.M., Yenush, L., Mulet, J.M., 2021. Identification of distinctive physiological and molecular responses to salt stress among tolerant and sensitive cultivars of broccoli (Brassica oleracea var. Italica). BMC plant biology 21, 1-16.
13. Chigumba, D.N., Mydy, L.S., de Waal, F., Li, W., Shafiq, K., Wotring, J.W., Mohamed, O.G., Mladenovic, T., Tripathi, A., Sexton, J.Z., Kautsar, S., 2022. Discovery and biosynthesis of cyclic plant peptides via autocatalytic cyclases. Nature Chemical Biology 18, 18-28.
14. Dou, C., Marcondes, W.F., Djaja, J.E., Bura, R., Gustafson, R., 2017 Can we use short rotation coppice poplar for sugar based biorefinery feedstock? Bioconversion of 2-year-old poplar grown as short rotation coppice. Biotechnology for biofuels 10, 1-15.
15. Fiehn, O., Kopka, J., Trethewey, R.N., Willmitzer, L., 2000. Identification of uncommon plant metabolites based on calculation of elemental compositions using gas chromatography and quadrupole mass spectrometry. Analytical chemistry 72, 3573-3580.
16. Fritsche-Guenther, R., Gloaguen, Y., Bauer, A., Opialla, T., Kempa, S., Fleming, C. A., Kirwan, J. A., 2021. Optimized workflow for on-line derivatization for targeted metabolomics approach by gas chromatography-mass spectrometry. Metabolites 11, 888
17. Gahoonia, T.S., Ali, R., Malhotra, R.S., Jahoor, A., Rahman, M.M., 2007. Variation in root morphological and physiological traits and nutrient uptake of chickpea genotypes. Journal of Plant Nutrition 30, 829-841.
18. Gall, H.L., Philippe, F., Domon, J.M., Gillet, F., Pelloux, J., Rayon, C., 2015. Cell wall metabolism in response to abiotic stress. Plants 4, 112-166.
19. Geng, P., Zhang, S., Liu, J., Zhao, C., Wu, J., Cao, Y., Zhao, Q., 2020. MYB20, MYB42, MYB43, and MYB85 regulate phenylalanine and lignin biosynthesis during secondary cell wall formation. Plant Physiology 182, 1272-1283.
20. Hamant, O., Pautot, V., 2010. Plant development: a TALE story. Comptes rendus biologies 333, 371-381.
21. Heise, K., Kontturi, E., Allahverdiyeva, Y., Tammelin, T., Linder, M. B., Nonappa, Ikkala, O., 2021. Nanocellulose: recent fundamental advances and emerging biological and biomimicking applications. Advanced Materials 33, 2004349

22. Heli, Z., Hongyu, C., Dapeng, B., Yee Shin, T., Yejun, Z., Xi, Z., Yingying, W., 2022. Recent advances of ɣ-aminobutyric acid: Physiological and immunity function, enrichment, and metabolic pathway. Frontiers in nutrition 9, 1076223.
23. Huang, J.H., Xu, J., Ye, X., Luo, T.Y., Ren, L.H., Fan, G.C., Qi, Y.P., Li, Q., Ferrarezi, R.S., Chen, L.S., 2019. Magnesium deficiency affects secondary lignification of the vascular system in Citrus sinensis seedlings. Trees 33, 171-182.
24. Huang, X.Y., Salt, D.E., 2016. Plant ionomics: from elemental profiling to environmental adaptation. Molecular plant 9, 787-797.
25. Hunter, J. D., 2007. Matplotlib: A 2D graphics environment. Computing in science & engineering 9, 90-95
26. Jervis, J., Hildreth, S.B., Sheng, X., Beers, E.P., Brunner, A.M., Helm, R.F., 2015. A metabolomic assessment of NAC154 transcription factor overexpression in field grown poplar stem wood. Phytochemistry 115, 112-120.
27. Jia, P., Yan, R., Wang, Y., Gao, F.H., Liu, Y., Dong, Q.L., Luan, H.A., Zhang, X.M., Li, H., Guo, S.P., Qi, G.H., 2024. Characterization of the KNOTTED1-like HOMEOBOX gene family in kiwifruit and functional analysis of AcKNOX11 related to plant growth, flowering, and melatonin-mediated germination inhibition. Scientia Horticulturae 325,112690.
28. Kumar, R., Bohra, A., Pandey, A.K., Pandey, M.K., Kumar, A., 2017. Metabolomics for plant improvement: status and prospects. Frontiers in Plant Science 8, 1302.
29. Legay, S., Lacombe, E., Goicoechea, M., Briere, C., Séguin, A., Mackay, J., Grima-Pettenati, J., 2007. Molecular characterization of EgMYB1, a putative transcriptional repressor of the lignin biosynthetic pathway. Plant Science 173, 542-549.
30. Legay, S., Sivadon, P., Blervacq, A.S., Pavy, N., Baghdady, A., Tremblay, L., Levasseur, C., Ladouce, N., Lapierre, C., Séguin, A., Hawkins, S., 2010. EgMYB1, an R2R3 MYB transcription factor from eucalyptus negatively regulates secondary cell wall formation in Arabidopsis and poplar. New phytologist 188, 774-786
31. Li ErYang, L. E., Wang ShuCai, W. S., Liu YuanYuan, L. Y., Chen JinGui, C. J., Douglas, C. J., 2011. OVATE FAMILY PROTEIN4 (OFP4) interaction with KNAT7 regulates secondary cell wall formation in Arabidopsis thaliana.
32. Li, E., Bhargava, A., Qiang, W., Friedmann, M.C., Forneris, N., Savidge, R.A., Johnson, L.A., Mansfield, S.D., Ellis, B.E., Douglas, C.J., 2012. The Class II KNOX gene KNAT7 negatively regulates secondary wall formation in Arabidopsis and is functionally conserved in *Populus*. New Phytologist 194, 102-115.
33. Liu, Q., Luo, L., Zheng, L., 2018. Lignins: biosynthesis and biological functions in plants. International journal of molecular sciences 19, 335.
34. Liu, Y., You, S., Taylor-Teeples, M., Li, W.L., Schuetz, M., Brady, S.M., Douglas, C.J., 2014. BEL1-LIKE HOMEODOMAIN6 and KNOTTED ARABIDOPSIS THALIANA7 interact and regulate

secondary cell wall formation via repression of REVOLUTA. The Plant Cell 26, 4843-4861.
35. Ma, R., Liu, B., Geng, X., Ding, X., Yan, N., Sun, X., Wang, W., Sun, X., Zheng, C., 2023. Biological function and stress response mechanism of MYB transcription factor family genes. Journal of Plant Growth Regulation 42, 83-95.
36. Marschner, H., 2011. Marschner's mineral nutrition of higher plants. Academic press.
37. McKinney, W., 2010. Data structures for statistical computing in Python. scipy 445, 51-56.
38. Mottiar, Y., Karlen, S.D., Goacher, R.E., Ralph, J., Mansfield, S.D., 2023. Metabolic engineering of p-hydroxybenzoate in poplar lignin. Plant Biotechnology Journal 21, 176-188.
39. Munns, R., Tester, M., 2008. Mechanisms of salinity tolerance. Annu. Rev. Plant Biology 59, 651-681.
40. Mydy, L.S., Chigumba, D.N., Kersten, R.D., 2021. Plant copper metalloenzymes as prospects for new metabolism involving aromatic compounds. Frontiers in plant science 12, 692108.
41. Pang, Z., Chong, J., Zhou, G., de Lima Morais, D. A., Chang, L., Barrette, M., Xia, J., 2021. MetaboAnalyst 5.0: narrowing the gap between raw spectra and functional insights. Nucleic acids research 49, W388-W396.
42. Pascual, M.B., El-Azaz, J., de la Torre, F.N., Cañas, R.A., Avila, C., Cánovas, F.M., 2016. Biosynthesis and metabolic fate of phenylalanine in conifers. Frontiers in plant science 7, 1030.
43. Pratelli, R., Pilot, G., 2014. Regulation of amino acid metabolic enzymes and transporters in plants. Journal of experimental botany 65, 5535-5556.
44. Qin, W., Yin, Q., Chen, J., Zhao, X., Yue, F., He, J., Yang, L., Liu, L., Zeng, Q., Lu, F., Mitsuda, N., 2020. The class II KNOX transcription factors KNAT3 and KNAT7 synergistically regulate monolignol biosynthesis in Arabidopsis. Journal of experimental botany 71, 5469-5483.
45. Ragauskas, A.J., Williams, C.K., Davison, B.H., Britovsek, G., Cairney, J., Eckert, C.A., Frederick Jr, W.J., Hallett, J.P., Leak, D.J., Liotta, C.L., Mielenz, J.R., 2006. The path forward for biofuels and biomaterials. Science 311, 484-489.
46. Rossum, V., 2009. Python 3 reference manual
47. Sahoo, D., Maiti, I., 2014. Biomass derived from transgenic tobacco expressing the Arabidopsis CESA3 ixr1-2 gene exhibits improved saccharification. Acta Biologica Hungarica 65, 189-204.
48. Sharma, P., Jha, A.B., Dubey, R.S., Pessarakli, M., 2021. Reactive oxygen species generation, hazards, and defense mechanisms in plants under environmental (abiotic and biotic) stress conditions. Handbook of plant and crop physiology. 617-658.
49. Shen, H., Yin, Y., Chen, F., Xu, Y., Dixon, R. A., 2009. A bioinformatic analysis of NAC genes for plant cell wall development in relation to lignocellulosic bioenergy production. BioEnergy Research 2, 217-232.

50. Taïbi, K., Del Campo, A.D., Vilagrosa, A., Bellés, J.M., López-Gresa, M.P., Pla, D., Calvete, J.J., López-Nicolás, J.M. Mulet., 2017. Drought tolerance in Pinus halepensis seed sources as identified by distinctive physiological and molecular markers. Frontiers in Plant Science 8, 1202.
51. Turner, M.F., Heuberger, A.L., Kirkwood, J.S., Collins, C.C., Wolfrum, E.J., Broeckling, C.D., Prenni, J.E., Jahn, C.E., 2016. Non-targeted metabolomics in diverse sorghum breeding lines indicates primary and secondary metabolite profiles are associated with plant biomass accumulation and photosynthesis. Frontiers in Plant Science 7, 953.
52. Wang, N., Ryan, L., Sardesai, N. et al., 2023. Leaf transformation for efficient random integration and targeted genome modification in maize and sorghum. Nat. Plants 9, 255–270
53. Wang, S., Yang, H., Mei, J., Liu, X., Wen, Z., Zhang, L., Xu, Z., Zhang, B., Zhou, Y., 2019. Rice homeobox protein KNAT7 integrates the pathways regulating cell expansion and wall stiffness. Plant physiology 181, 669-682.
54. Wang, Y., Chen, Y.F., Wu, W.H., 2021. Potassium and phosphorus transport and signaling in plants. Journal of Integrative Plant Biology 63, 34-52.
55. Xie, Y., Zheng, K., Chen, Y., Li, J., Guo, J., Cao, J., Zhu, M., 2025. In Vitro Plantlet Regeneration and Accumulation of Ginkgolic Acid in Leaf Biomass of Ginkgo biloba L. Forests 16, 1539
56. Xu, C., Fu, X., Liu, R., Guo, L., Ran, L., Li, C., Tian, Q., Jiao, B., Wang, B., Luo, K., 2017. PtoMYB170 positively regulates lignin deposition during wood formation in poplar and confers drought tolerance in transgenic Arabidopsis. Tree physiology 37,1713-1726.
57. Xu, E., Liu, Y., Gu, D., Zhan, X., Li, J., Zhou, K., Zhang, P., Zou, Y., 2024. Molecular Mechanisms of Plant Responses to Copper: From Deficiency to Excess. International journal of molecular sciences 25, 6993.
58. Xu, W., Zhao, Y., Liu, Q., Diao, Y., Wang, Q., Yu, J., Liu, B., 2023. Identification of ZmBK2 Gene Variation Involved in Regulating Maize Brittleness. Genes 14, 1126
59. Yadav, S., Chattopadhyay, D., 2023. Lignin: the building block of defense responses to stress in plants. Journal of Plant Growth Regulation 42, 6652-6666.
60. Yamaguchi, M., Sato, A., Takahashi, D., Mori, K., Fujimoto, R., Miyagi, A., Kotake, T., 2025. The rice BRITTLE CULM 4 gene encodes a membrane protein affecting cellulose synthesis in the secondary cell wall. Plant and Cell Physiology 66, 1444-1453.
61. Yao, W., Zhang, D., Zhou, B., Wang, J., Li, R., 2020. Over-expression of *poplar* NAC15 gene enhances wood formation in transgenic tobacco. BMC Plant Biology 20, 12.
62. Ye, X., Huang, H.Y., Wu, F.L., Cai, L.Y., Lai, N.W., Deng, C.L., Guo, J.X., Yang, L.T., Chen, L.-S., 2021. Molecular mechanisms for magnesium-deficiency-induced leaf vein lignification, enlargement

and cracking in Citrus sinensis revealed by RNA-Seq. Tree Physiology 41, 280–301.
63. Yener, I., Temel, H., Tokul-Olmez, O., Firat, M., Oral, E.V., Akdeniz, M., Senturk, K., Kaplaner, E., Ozturk, M., Ertaş, A., 2019. Trace element analysis by icp-ms and chemometric approach in some euphorbia species: Potential to become a biomonitor. Iranian Journal of Pharmaceutical Research: IJPR 18, 1704.
64. Zhang, Y., Huang, B., Jin, J., Xiao, Y., Ying, H., 2023. Recent advances in the application of ionomics in metabolic diseases. Frontiers in Nutrition 9, 1111933.
65. Zhao, K., Bartley, L.E., 2014. Comparative genomic analysis of the R2R3 MYB secondary cell wall regulators of Arabidopsis, poplar, rice, maize, and switchgrass. BMC plant biology 14, 1-21.
66. Zhong, R., Lee, C., Ye, Z.H., 2010. Functional characterization of poplar wood-associated NAC domain transcription factors. Plant Physiology 152, 1044-1055.
67. Zhong, R., Richardson, E.A., Ye, Z.H., 2007. Two NAC domain transcription factors, SND1 and NST1, function redundantly in regulation of secondary wall synthesis in fibers of Arabidopsis. Planta 225, 1603-1611.
68. Zhu, Q., Wu, Y., Zhang, X., Xu, N., Chen, J., Lyu, X., Zeng, H., Yu, F., 2024. Metabolomic and transcriptomic analyses reveals candidate genes and pathways involved in secondary metabolism in Bergenia purpurascens. BMC genomics 25,1083.